Title: Modulation of kinesin's load-bearing capacity by force geometry and the microtubule track

Authors: Serapion Pyrpassopoulos[1,*], Henry Shuman[1], E. Michael Ostap[1,*].

Affiliations:

[1]Pennsylvania Muscle Institute, Department of Physiology, and the Center for Engineering Mechanobiology, University of Pennsylvania, Perelman School of Medicine, Philadelphia, PA, US.

[*]Correspondence should be addressed to serappyr@pennmedicine.upenn.edu or ostap@pennmedicine.upenn.edu

Abstract:

Kinesin motors and their associated microtubule tracks are essential for long-distance transport of cellular cargos [1]. Intracellular activity and proper recruitment of kinesins is regulated by biochemical signaling, cargo adaptors and microtubule associated proteins[2–4]. Here we report on a novel regulatory mechanism of kinesin's load-bearing capacity by forces across the microtubule track. Using optical tweezers and the three-bead assay[5,6] to specifically apply forces parallel to the long-axis of the microtubule, we found that the median attachment duration between kinesin and microtubules under opposing forces is up to 10-fold longer than observed previously using the more conventional single-bead assay, which is likely due to vertical forces imposed by the single bead [7]. Using the three-bead assay, we also found that not all the protofilaments are equivalent interacting substrates for kinesin and that the median attachment duration of kinesin varies by more than 10-fold, depending on the relative angular position of the forces along the circumference of the microtubule. Thus, depending on the geometry of forces across the microtubule, kinesin can switch from a fast detaching motor (< 0.2 s) to a persistent motor that sustains attachment (> 3 s) at high forces (5 pN). Our data show that the load-bearing capacity of the kinesin motor is highly variable and can be dramatically affected by off-axis forces and forces across the microtubule lattice which has implications for a range of cellular activites including cell division and organelle transport.

Main Text:

Microtubules are cytoskeletal filaments essential for long-distance transport of intracellular cargos towards their plus and minus ends via kinesin and dynein motors, respectively [1]. The stepping behavior of kinesin has been studied in detail at the single molecule level, both in the presence and in the absence of external loads on the motor [8–14]. For most purposes, microtubules have been assumed to be passive tracks for motility that stimulate kinesin's ATPase activity. However, mounting evidence suggests that kinesin binding to microtubules may result in conformational changes in the microtubule lattice that result in kinesin's cooperative binding [15–17]. Notably, GDP-microtubules elongate 1.3 - 1.6 % when interacting with saturating concentrations of kinesin-1 [18,19]. Implicit in these experiments and their interpretation is the concept of structural plasticity of the microtubule lattice playing a role in microtubule function [20]. Recent theoretical work suggests that kinesin-induced asymmetric shear deformation of the microtubule lattice may be the mechanism of cooperative kinesin binding [21]. To determine directly if external shear forces on the microtubule lattice affect the mechanosensitivity of kinesin molecules, we used optical tweezers to impart mechanical forces on microtubules during processive kinesin stepping (Fig. 1).

We first examined the effect of assay geometry on the duration of kinesin attachment in the presence of mechanical load, since recent theoretical work[7] proposed that the well-established single-bead optical trapping assay [8] applies forces to kinesin that are vertical to the microtubule long axis, resulting in the acceleration of detachment. Additionally, we checked if different substrates and/or microtubule surface-attachment strategies have any effect on the mechanical activity of a two-headed kinesin-1 construct

[22] (Supplementary Information). Kinesin molecules were site-specifically bound to beads (dia. = 0.82 or 0.61 μm, Supplementary Information) which were held in a stationary optical trap as kinesin stepped along taxol-stabilized GDP-microtubules attached to (a) a solid surface via tubulin antibody or via streptavidin bound to biotinylated microtubules, or (b) a biotinylated supported lipid bilayer via streptavidin bound to biotinylated microtubules (Supplementary Information). As kinesin walks along the microtubule and pulls the bead away from the center of the trap, the force on the kinesin increases until kinesin detaches from the microtubule (Fig. 1a), resulting in the bead moving rapidly back to the center of the trap before the motor reengages to start another processive run. The force at detachment (F_{detach}) and the duration of attachment (Δt) at 2 mM MgATP were measured for each run (Fig. 1c). Representative measurements for different surfaces are shown in Fig. 2e and Fig 2i; Supplemental Table 1). From 20 different pairs of beads and microtubules, the median Δt < 1 s, and the average $\langle F_{detach} \rangle$ of 2087 runs was 4.2 ± 1.5 pN (SD: standard deviation), in good agreement with a previously measured value of 4.4 ± 1.4 pN [23] and an estimated characteristic value of 3.7 pN [13]. To test if the lack of attachments along the microtubule segment that interacts with kinesin may lead to different behavior, we fabricated parallel rectangular pedestal ridges (4 mm long, 2 μm wide, 1 μm tall and 10 μm apart; Supplementary Information and Supplementary Video 1). Microtubules were immobilized across the top and perpendicular to the long axis of the ridges, resulting in a geometry similar to the dumbbell (Supplemental Fig. 1, Supplemental Video 1).The single bead assay with microtubules suspended between rectangular ridges revealed similar values to those of the surface-immobilized

microtubules (<F_{detach} > = 3.1 ± 1.9 pN (SD, n = 432 runs); (<median-Δt >$_w$ = 0.30 ± 0.11 s (SD_w, n = 7)) (Fig. 2f & 2j).

To apply variable tensile forces on a microtubule while interacting with kinesin and reduce the effect of the force component vertical to the microtubule axis, which is inherent to the single-bead assay[7], we used a dual laser trap and the three-bead assay (Fig. 1). The three-bead assay has been used mostly for single molecule studies of the non-processive actomyosin complex [6] and less frequently for microtubule interacting motors[24–26]. Two streptavidin-coated polystyrene beads (dia. = 0.82 μm), trapped by two laser beams ~10 um apart, were brought in contact with a taxol-stabilized biotinylated GDP-microtubule in solution until a stable "dumbbell" assembly was formed (Fig. 1b). Initial pretensile force ($F_{pretensile}$ = 2-9 pN) was applied to the dumbbells by moving the two laser beams further apart. Kinesin molecules were anchored on surface-immobilized spherical pedestals (dia. = 2.5 um) against which microtubule dumbbells were brought in contact. Single molecule kinesin motility resulted in the displacement of the dumbbells relative to the surface immobilized kinesin. Single kinesin molecules (Supplementary Information; Supplemental Fig. 2) interacting with microtubule dumbbells in the presence of 2 mM MgATP reached forces ≥ 5 pN more frequently and remained attached at these high forces remarkably longer than observed in the single-bead assay (Fig 1d). Representative examples of the distribution and statistics of Δt and F_{detach} between kinesin and different microtubule dumbbells are shown in Fig. 2g and Fig. 2k, correspondingly. The median duration of the runs produced by kinesin varied for different dumbbells by more than an order of magnitude (0.14 s and 3.8 s) and followed a bell shape distribution (Fig. 2m) with a weighted mean (Supplementary Information) of <median-Δt >$_w$ = 1.3 ± 0.59 s (SD_w:

weighted standard deviation, n = 50). Single beads interacting with surface-immobilized microtubules didn't demonstrate such a variability and the corresponding value was $\langle \text{median-}\Delta t \rangle_w = 0.34 \pm 0.083$ s (SD_w, n = 20) (Fig. 2m). The average F_{detach} for dumbbells was 42 % higher than the corresponding average for surface immobilized microtubules (6.0 ± 1.8 pN vs. 4.2 ± 1.5 pN; SD; $p < 0.05$ Mann-Whitney test; n = 5343 and 2087 runs, respectively) (Supplemental Fig. 3). Although median-Δt and $\langle F_{detach} \rangle$ changed significantly, during the initial motility phase ($F_{detach} \leq 3$ pN) the weighted mean of the average velocity of kinesin between the single-bead and three-bead assays differed by less than 10% (300 ± 65 nm/s vs. 280 ± 83 nm/s, respectively; Supplemental Fig. 4). Similar differences between microtubule dumbbells and surface-immobilized microtubules, were observed when GMPCPP was used instead of GTP and taxol to produce stable microtubules (Supplemental Fig. 5). This result suggests that the broad variability of median-Δt observed in the three-bead assay (Fig. 2m) is not due to the variability in microtubule protofilament number [27,28].

The distribution of Δt between a single kinesin and a given dumbbell did not show dependence on the magnitude of the tensile forces between 2 - 9 pN applied on the dumbbell (Supplemental Fig. 6). Additionally, when no tensile forces were applied and only the one bead attached to the plus-end of the microtubule was trapped, kinesin achieved the high forces (Fig. 2d) and long dwell times observed for dually trapped dumbbells (Fig. 2l). Note that for most of the dumbbells $\langle F_{detach} \rangle$ (~ 6 pN) was greater than $F_{pretensile}$ (~4 pN). To test if the broad distribution of median-Δt (Fig. 2m) is due to kinesins processing along microtubules not parallel to the coverslip (Supplemental Fig. 7a), we tested the sensitivity of the Δt-distribution for a given dumbbell to changes in *z*-

displacement. Increasing by 50 or 100 nm the separation along the z-axis between a given dumbbell and the kinesin changed only the probability of kinesin attachment, but not the Δt-distribution (Supplemental Fig. 8b, c, d, e). However, the z-force developed in the single bead assay is expected to be larger (~ 25 pN) than in the three-bead assay (~0.4 pN; Supplemental Fig. 7). This larger force has been proposed to accelerate the forced detachment kinetics of kinesin[7] and lead to a narrow distribution of median-Δt, as we see in our experiments (Figure 2m).

The most variable experimental parameter among the dumbbells in the three-bead assay is the geometry of shear forces (Supplemental Fig. 9). When microtubule dumbbells are formed, the trapped beads do not always bind at the same azimuthal position relative to each other or the surface-immobilized kinesin molecule. Therefore, the relative azimuthal positions of the pair of opposing forces between the interacting kinesin and the plus-end trapped bead will be variable in the three-bead assay (Supplemental Video 2). If this angular variability is responsible for the broad distribution of attachment durations at (Fig. 2m), then the values median-Δt_1 and median-Δt_2 of kinesin interacting at diametrically opposite positions along the cross section of the same microtubule dumbbell should be different.

To test this proposal, we collected two data sets for each dumbbell (n = 24 dumbbells). First the dumbbell was brought into contact with a pedestal on the bottom of the experimental chamber, and then to a pedestal on top of the same chamber (Fig. 3a). By testing this pair of interactions, we are probing diametrically opposite sides of the microtubule, and thus changing the angle φ (Fig. 3b). We found the median-Δt_1 for pedestals on the bottom and median-Δt_2 for pedestals on the top to be anti-correlated

with a Pearson coefficient of -0.5 ($p = 0.02$). Note that the short and long interactions did not always occur on the same side of the chamber, but were rather random, arguing against a systematic artifact causing the anti-correlation (Fig. 3c). Indeed the distributions of median-Δt_1 and median-Δt_2 are similar to each other (Fig. 3d) and to the distribution in Fig. 2m.

To establish that the anti-correlation between median-Δt_1 and median-Δt_2 was due to a significant change of the relative azimuthal position, φ, we performed experiments this time testing the same dumbbell ($n = 17$) against two different pedestals on the same side of the experimental chamber (Fig. 3b and 3e). In contrast to the experiment above, the Pearson correlation coefficient for median-Δt_1 and median-Δt_2 is positive 0.7 ($p = 0.001$) (Fig 3f). It is likely that the actual values of both correlation and anti-correlation coefficients are underestimated because we do not have a fine positional control at the protofilament level. The azimuthal position φ will not always be exactly the same for spherical pedestals across the same surface (Fig. 3f) and not always exactly π-φ for spherical pedestals in opposing surfaces (Fig 3b).

Our results show that the attachment duration and the magnitude of opposing forces that can be sustained by the microtubule-kinesin complex, or else kinesin's load-bearing capacity, is highly variable and can be dramatically affected by the geometry of forces relative to its microtubule track. For different cellular processes in which the microtubule-kinesin complex can be subject to opposing forces such as during cargo transport and mitotic division the 3D orientation of the force vector can be significantly different between the two cases. A significant difference in the force vector due to the presence of a larger force component vertical to the microtubule in the single-bead assay

relative to three-bead assay is most likely the reason for the observed differences in <median-Δt > of the microtubule-kinesin complex between the two assays, supporting a recent theoretical study[7]. Moreover, when opposing forces are oriented mainly along the microtubule axis (dumbbell assay), kinesin's load-bearing capacity depends on the relative angular position of the pairs of opposing forces around the circumference of the microtubule. Depending on its location on the microtubule, kinesin can switch from a fast detaching motor to a persistent motor that can sustain its microtubule attachment at high forces (>5 pN) for extended lengths of time, with almost an order of magnitude difference. The mechanism for the observed variability of kinesin's load-bearing capacity in the three-bead assay is likely related to the structural plasticity of the microtubule and/or possible cooperative clustering of different post-translationally modified tubulin isoforms during microtubule polymerization, such that not all the protofilaments of a microtubule are equivalent interacting substrates for kinesin under opposing forces. Nevertheless, our findings point to a more general mechanism by which the duration of the interaction between microtubules and binding partners can be a more complex function of the geometry of forces than previously appreciated.

Methods.

Full list of all the reagents and methods are contained in the Supplementary Information.

References.

1. Caviston, J. P. & Holzbaur, E. L. F. Microtubule motors at the intersection of trafficking and transport. *Trends Cell Biol.* **16,** 530–537 (2006).

2. Akhmanova, A. & Iii, J. A. H. Linking molecular motors to membrane cargo. *Curr. Opin. Cell Biol.* **22,** 479–487 (2010).

3. Song, Y. & Brady, S. T. Post-translational modifications of tubulin : pathways to functional diversity of microtubules. *Trends Cell Biol.* **25,** 125–136 (2015).

4. Sirajuddin, M., Rice, L. M. & Vale, R. D. Regulation of microtubule motors by tubulin isotypes and post-translational modifications. *Nat. Cell Biol.* **16,** (2014).

5. Finer, J. T., Simmons, R. M. & Spudich, J. A. Single myosin molecule mechanics: piconewton forces and nanometer steps. *Nature* **368,** 113 (1994).

6. Laakso, J. M., Lewis, J. H., Shuman, H. & Ostap, E. M. Myosin I Can Act As a Molecular Force Sensor. *Science.* **321,** 133–136 (2008).

7. Khataee, H. & Howard, J. The Force Generated by Two Kinesin Motors Depends on Load Direction and Intermolecular Coupling. *Phys. Rev. Lett.* **Submitted,** (2019).

8. Svoboda, K. & Block, S. M. Force and velocity Measured for Single Kinesin Molecules. *Cell* **77,** 773–784 (1994).

9. Meyhofer, E. & Howard, J. The force generated by a single kinesin molecule against an elastic load. *Proc. Natl. Acad. Sci.* **92,** 574–578 (1995).

10. Coppin, C. M., Pierce, D. W., Hsu, L. & Vale, R. D. The load dependence of kinesin ' s mechanical cycle. *Proc. Nat. Acad. Sci. USA* **94,** 8539–8544 (1997).

11. Kojima, H., Muto, E., Higuchi, H. & Yanagida, T. Mechanics of single kinesin molecules measured by optical trapping nanometry. *Biophys. J.* **73,** 2012–2022 (1997).

12. Visscher, K., Schnitzer, M. J. & Block, S. M. Single kinesin molecules studied with

a molecular force clamp. *Nature* **400,** 184–189 (1999).

13. Schnitzer, M. J., Visscher, K. & Block, S. M. Force production by single kinesin motors. *Nat. Cell Biol.* **2,** 718–723 (2000).

14. Clancy, B. E., Behnke-Parks, W. M., Andreasson, J. O. L., Rosenfeld, S. S. & Block, S. M. A universal pathway for kinesin stepping. *Nat. Struct. Mol. Biol.* **18,** 1020–1027 (2011).

15. Vilfan, A. *et al.* Dynamics and cooperativity of microtubule decoration by the motor protein kinesin. *J. Mol. Biol.* **312,** 1011–1026 (2001).

16. Muto, E., Sakai, H. & Kaseda, K. Long-range cooperative binding of kinesin to a microtubule in the presence of ATP. *J. Cell Biol.* **168,** 691–696 (2005).

17. H Roos, W. *et al.* Dynamic kinesin-1 clustering on microtubules due to mutually attractive interactions. *Phys. Biol.* **5,** (2008).

18. Peet, D. R., Burroughs, N. J. & Cross, R. A. Kinesin expands and stabilizes the GDP-microtubule lattice. *Nat. Nanotechnol.* **13,** 386–391 (2018).

19. Shima, T. *et al.* Kinesin-binding–triggered conformation switching of microtubules contributes to polarized transport. *J. Cell Biol.* jcb.201711178 (2018). doi:10.1083/jcb.201711178

20. Kueh, H. Y. & Mitchison, T. J. Structural Plasticity in Actin and Tubulin Polymer Dynamics. *Science.* **325,** 960–964 (2009).

21. Sekimoto, K. & Prost, J. Elastic anisotropy scenario for cooperative binding of kinesin-coated beads on microtubules. *J. Phys. Chem. B* **120,** 5953–5959 (2016).

22. Pierce, D. W. & Vale, R. D. Assaying Processive Movement of Kinesin by Fluorescence Microscopy. *Methods Enzymol.* **298,** 154–171 (1998).

23. Schroeder, H. W. *et al.* Force-dependent detachment of kinesin-2 biases track switching at cytoskeletal filament intersections. *Biophys. J.* **103,** 48–58 (2012).

24. Walter, W. J., Brenner, B. & Steffen, W. Cytoplasmic dynein is not a conventional processive motor. *J. Struct. Biol.* **170,** 266–269 (2010).

25. Butterfield, A. E., Stewart, R. J., Schmidt, C. F. & Skliar, M. Bidirectional Power Stroke by Ncd Kinesin. *Biophysj* **99,** 3905–3915 (2010).

26. Walter, W. J., Koonce, M. P., Brenner, B. & Steffen, W. Two independent switches regulate cytoplasmic dynein ' s processivity and directionality. *Proc. Nat. Acad. Sci. USA* **109,** 1–5 (2012).

27. Hyman, A. A., Chretien, D., Arnal, I. & Wade, R. H. Structural Changes Accompanying GTP Hydrolysis in Microtubules: Information from a Slowly Hydrolyzable Analogue Guanylyl-(c ,/3)-Methylene-Diphosphonate. *J. Cell Biol.* **128,** 117–125 (1995).

28. Dıaz, J. F., Valpuesta, J. M., Chacon, P., Diakun, G. & Andreu, J. M. Changes in Microtubule Protofilament Number Induced by Taxol Binding to an Easily Accessible Site. *J. Biol. Chem.* **273,** 33803–33810 (1998).

Acknowledgments: The authors would like to thank Aaron Snoberger for careful reading of the manuscript. **Funding**: NIH grant GM087253 to H.S and E.M.O, and NSF Science and Technology Center, CMMI: 15-48571to E.M.O.

Author Contributions: S.P., H. S. and E.M.O. designed the experiments. S.P. performed the experiments and analyzed the data. S.P., H.S. and E.M.O. wrote the manuscript.

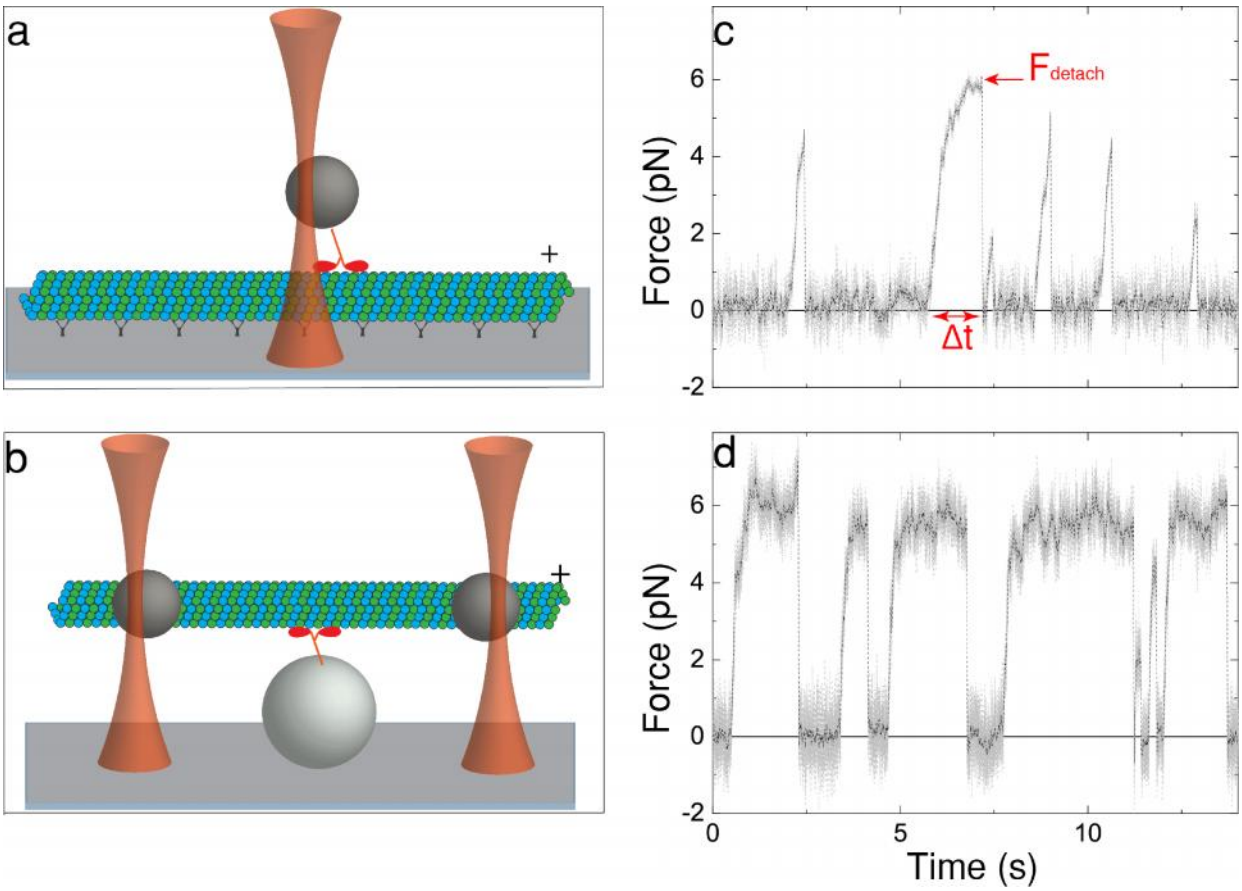

Fig. 1. Single and three-bead assays for kinesin-microtubule interaction. Cartoon representations (not drawn to scale) of (a) the single-bead assay and (b) the three-bead assay. (a) A microtubule (green and blue) is immobilized on a glass coverslip (gray surface) via antibody or streptavidin (black). A kinesin molecule (red) attached on a bead (gray sphere) is brought into contact via optical tweezers (brown). (b) A microtubule is attached to two laser-trapped beads via streptavidin-biotin linkage. The microtubule-assembly (microtubule dumbbell) is brought in contact with a single kinesin molecule, attached on surface-immobilized spherical pedestal. Representative raw (gray) and smoothed (black) force traces of a single kinesin molecule interacting with (c) a surface-immobilized microtubule in the single-bead assay and (d) a microtubule dumbbell in the three-bead assay. The force (F_{detach}) at which the kinesin detaches (red arrow in (c)) from

the microtubule and the duration Δt of the corresponding force ramp (double red arrow in (c)) can be calculated directly from the data for every force ramp.

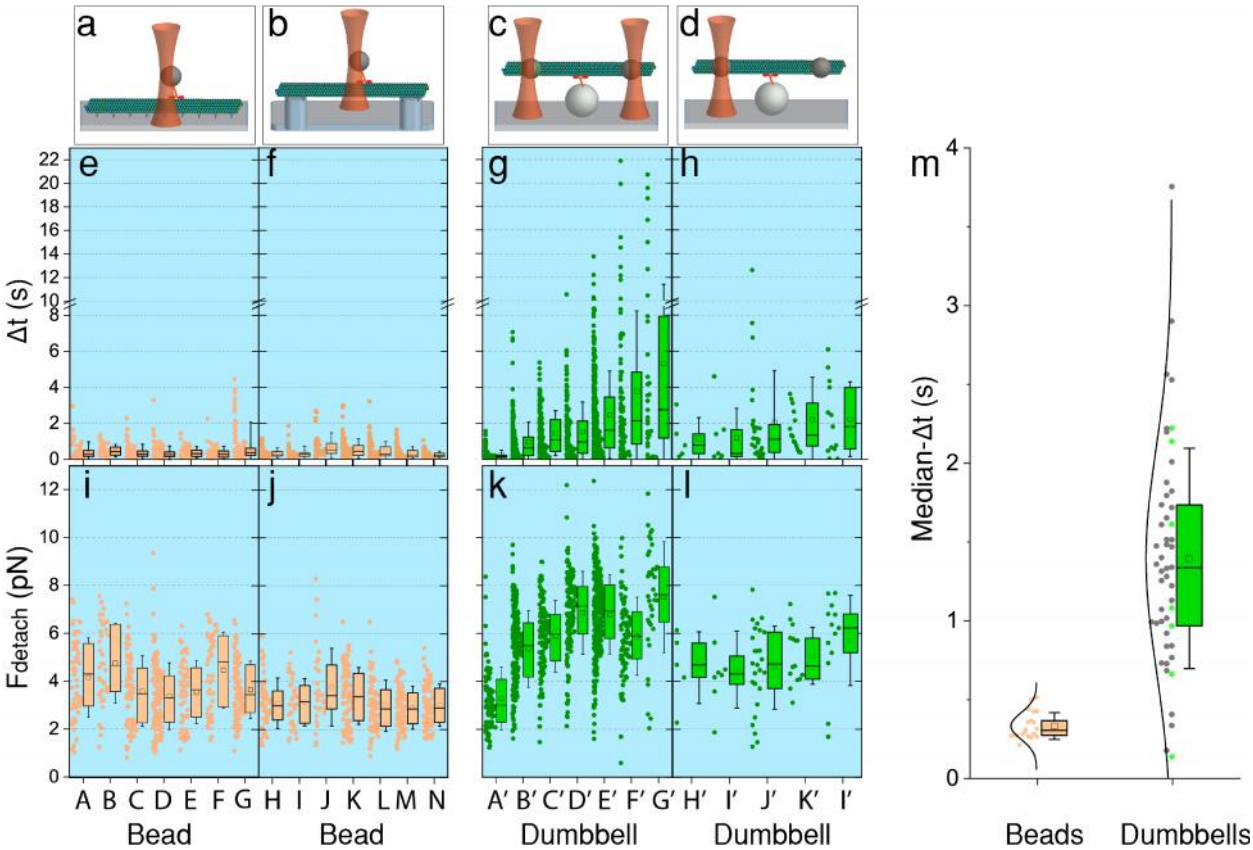

Fig. 2. Kinesin's attachment durations and detachment forces for single and three-bead assays. Cartoon descriptions for each assay are shown on plots (a), (b), (c) and (d). Representative distributions of Δt and F_{detach} and their corresponding box-statistics for: (e, i) different pairs of beads (A to G) and surface immobilized microtubules (Extended Data Table 1); (f, j) different microtubule dumbbells (A' to G'); (g, k) different pairs of beads (H to N) and microtubules suspended between rectangular ridges and (h, l) microtubule dumbbells (H' to I') laser trapped only by the bead at plus end and interacting with single kinesin. For each box the width corresponds to the inter-quartile range (IQR), the error bars to standard deviation (SD), the mid-line to the median value and the square inside each box to the average value. (m) The distribution and box statistics of the median-Δt for single kinesin molecules interacting with microtubule dumbbells (n = 50) and surface-

immobilized microtubules (n = 20) under resisting load. The green points correspond to the examples shown in plot (g). The black lines, which mainly serve as a guide to the eye, represent a normal distribution with the same mean and standard deviation as the corresponding data.

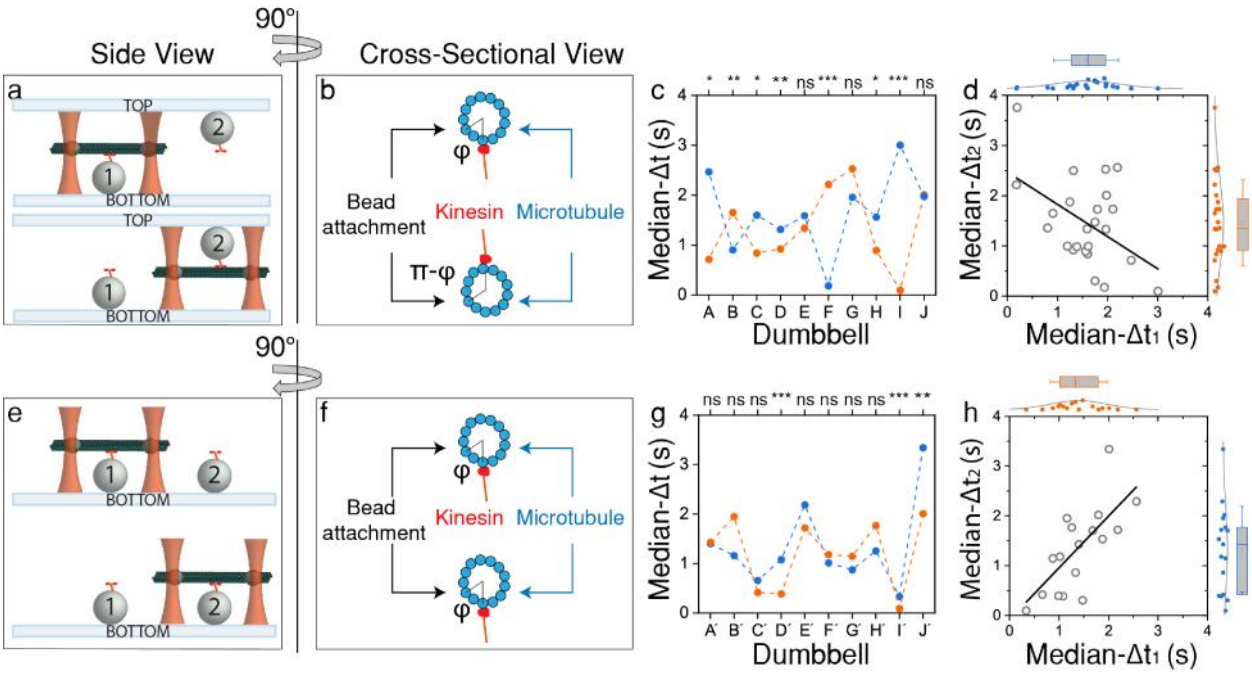

Fig. 3. The interaction between kinesin and microtubule dumbbells depends on the relative azimuthal position ¨ of opposing forces. Cartoon representation of experiments in which the same dumbbell is brought against two different interacting pedestals "1" and "2" (a, b) in opposing surfaces (top and bottom) or (e, f) along the same surface. In (b) and (f) φ or π-φ indicate the relative azimuthal position between the attached bead and the interacting kinesin. Plots of median-Δt for 10 different microtubule dumbbells against two different pedestals (Δt_1, Δt_2): (c) on the top and bottom surface and (g) along the same surface of the experimental chamber. Dumbbells "I" and "J" in plot (c) are the same with dumbbells "I′" and "J′", respectively, in plot (g). The statistical significance of the difference between median-Δt_1 and median-Δt_2 for each dumbbell is shown on top of plots (c) and (g) (Mann-Whitney test; ns = not significant, * stands for $p < 0.05$, ** for $p<0.01$, *** for $p<0.001$). (d) and (h) are scatter plots of median-Δt_1 and median-Δt_2 and solid lines represent linear fits. The distribution and statistics of median-

Δt_1 and median-Δt_2 are plotted on the top and the right, respectively, of the plots (d) and (h).